HIGH ACCURACY SPACE STRUCTURES MONITORING
BY A CLOSE-RANGE PHOTOGRAMMETRIC NETWORK

Jafar Amiri Parian (1), Armin Gruen (1), Alessandro Cozzani (2)

(1) Institute of Geodesy and Photogrammetry, ETH Zurich
(2) European Space Technology and Research Center (ESTEC)
Email: (j.amiriparian, agruen)@geod.baug.ethz.ch
alessandro.cozzani@esa.int

Commission V, WG 1

KEY WORDS: Network Design, Camera Calibration, Deformation Monitoring, Best-fit Ellipsoid, Accuracy

ABSTRACT:

The Planck mission of the European Space Agency (ESA) is designed to image the anisotropies of the Cosmic Background Radiation Field over the whole sky. To achieve this aim, sophisticated reflectors are used as part of the Planck telescope receiving system. The system consists of secondary and primary reflectors which are sections of two different ellipsoids of revolution with mean diameters of 1 and 1.6 meters. Deformations of the reflectors which influence the optical parameters and the gain of receiving signals are investigated in vacuum and at very low temperatures. For this investigation, among the various high accuracy measurement techniques, photogrammetry was selected. With respect to the photogrammetric measurements, special considerations should be taken into account in different steps of design and processing, such as determinability of additional parameters under the given network configuration, datum definition, reliability and precision issues as well as workspace limits and propagating errors from different sources. We have designed an optimal close-range photogrammetric network by heuristic simulation for the primary and secondary reflectors with a relative precision better than 1:1,000,000 to achieve the requested accuracies. A least squares best-fit ellipsoid was developed to determine the optical parameters of the reflector. In this paper we will report about our network design and the results of real measurements based on the tests executed by Alcatel Alenia Space France (AASF) under European Space Technology and Research Center (ESTEC) contract in vacuum and under very low temperatures.

1. INTRODUCTION

The Planck mission will collect and characterise radiation from the cosmic microwave background using sensitive radio receivers operating at extremely low temperatures. Planck's objective is to analyze, with the highest accuracy ever achieved, the remnants of the radiation that filled the universe immediately after the Big Bang, which we observe today as the Cosmic Microwave Background (CMB). Planck was selected as the third Medium-Sized Mission (M3) of ESA's Horizon 2000 scientific program, and is today part of its Cosmic Vision program. It is designed to image the anisotropies of the cosmic background radiation field over the whole sky, with unprecedented sensitivity and angular resolution. Planck will help provide answers to one of the most important sets of questions asked in modern science - how did the universe begin, how did it evolve to the state we observe today, and how will it continue to develop in the future? The Planck mission will collect and characterise radiation from CMB using sensitive radio receivers. These receivers will determine the black body equivalent temperature of the background radiation and will be capable of distinguishing temperature variations of about one micro-Kelvin. These measurements will be used to produce the best ever maps of anisotropies in the CMB radiation field.

To achieve this aim well-manufactured reflectors are used as part of the Planck telescope receiving system (Figure 1). The telescope consists of the Secondary Reflector (SR) and the Primary Reflector (PR) which are specific sections of two different ellipsoids of revolution with mean aperture size of 1 meter and 1.6 meters. Deformations of the reflectors which influence the optical parameters and the gain of the received

signals are investigated in vacuum and at low temperatures (down to 95 Kelvin) to investigate the correlation of the thermoelastic model used in its design with the actual performance. Surface accuracy and optical parameters (radius of curvature and conic constant) and their precisions are requested parameters defined by ESA-ESTEC[*].

For the deformation monitoring of the reflectors the concept of hyper-image digital photogrammetry was used in design and practice. This is based on extremely high network redundancy and the modeling of all possible systematic errors. Based on the designed photogrammetric networks real tests were executed by AASF[**] under ESA-ESTEC contract. In this paper we will present our procedure of different steps of design and the results of real measurement of the Planck Primary Reflector Flight Model (PRFM) which indicates an overall precision better than 1:1,000,000.

2. DESIGN STEPS

For the sake of simplicity, the design problem was divided into three sub-problems according the concept of network design, which was proposed by Grafarend, 1974:

1) Second Order Design (SOD)
   To relate 3D point coordinates with optical parameters of the reflector, best-fit ellipsoid was developed and based on it, SOD was performed to determine the required precision of the

---

[*] http://www.esa.int/esaCP/SEMOMQ374OD_index_0.html
[**] http://www.alcatel.com/space/index.htm

point coordinates with respect to the requested optical parameters.

2) Zero Order Design (ZOD)

To choose a suitable datum in order to achieve best possible precision for the optical parameters.

3) First Order Design (FOD)

A close-range photogrammetric network was designed by heuristic simulation in order to obtain the precision of the point coordinates which matches the estimated precision of the first step (SOD).
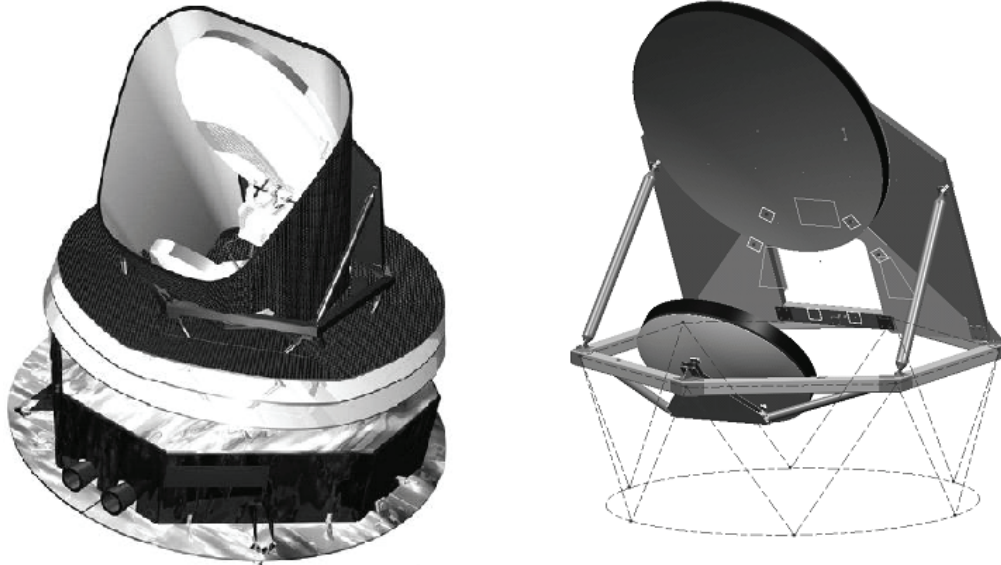
Figure 1. Planck Telescope (left). The telescope structure (right) with primary reflector (top) and secondary reflector (bottom), (Courtesy of Alcatel Alenia Space).

2.1. Best-Fit Ellipsoid and Second Order Design

The PR is a section of an ellipsoid of revolution around a Z-axis with a and b as principal axes (Equation 1).

$$\frac{X^2}{b^2} + \frac{Y^2}{b^2} + \frac{Z^2}{a^2} = 1 \qquad (1)$$

The optical parameters of PR are computed by equations (2) and (3):

$$K = E^2, \text{ with } E = \sqrt{1 - \frac{b^2}{a^2}} \qquad (2)$$

$$R = a(1 - E^2) \qquad (3)$$

In which K, R and E are the conic constant, the radius of curvature and the eccentricity.

Equation (1) is a standard form of an ellipsoid of revolution with aligned principal axes to the axes of the coordinate system and the ellipsoid center at the origin. In the case of a different coordinate system of the point cloud with respect to the coordinate system of the ellipsoid, an appropriate transformation is used for mapping the point cloud to the ellipsoid coordinate system.

The solution is achieved by a combined model of least squares fitting of an ellipsoid to the measured point cloud.

The requested accuracies are related to the optical parameters of the PR which were defined by ESA-ESTEC. These parameters cannot be measured directly with photogrammetry. Therefore points on the surface of the PR are measured and the optical parameters are estimated using the mentioned best-fit ellipsoid method. These points in our case are the centers of circular retro-reflective targets.

The distribution of targets, the number and accuracy of the point coordinates are the factors that influence the precision of the optical parameters. Since the PR is a section of an ellipsoid it has different curvatures in different areas. Therefore the targets have to be distributed such that there exist a sufficient number in areas of higher curvature. In addition, the increase of the number of points improves the precision of the optical parameters. The precision of the 3D points is also a large factor influencing the precision of the optical parameters.

Since the configuration is known, the problem in this step is to decide the weights of the observations (point coordinates) to meet the design criteria. The precision values of the observations are estimated by SOD. In other words, the weight matrix of observations, which are X, Y and Z coordinates, are estimated from the covariance matrix of unknowns, which are the optical parameters. For strong geometrical networks with a relatively large number of targets, it can be assumed that this weight matrix is a diagonal matrix. The solution of SOD is selected based on the method which estimates the diagonal of the weight matrix. It is an iterative method proposed by Wimmer, 1982 and is a direct approximation of the weight matrix based on Q_{XX} (cofactor matrix of point coordinates).

However, to be sure that the diagonal weight matrix, which is constructed by the estimated precision of the point coordinates from SOD is fulfilling the requirements, an error propagation was done to estimate the precision of the optical parameters.

In addition, the target thickness and the ambiguity of target thickness were modeled in the best-fit ellipsoid for the error propagation. Considering the potential accuracy of the photogrammetric method and the possible number of targets that could be stuck on the surface of the PR, successful results were achieved by using approximately 1000 targets that were distributed homogeneously on the surface of the PR. A homogeneous distribution of targets makes target sticking easier and needs less effort with respect to other target maps (inhomogeneous distributions).

2.2. Datum Definition

For an accurate estimation of the optical parameters appropriate datums were selected. Two datum choices were used for the estimation of these parameters:

1. An inner constraints datum for resolving 7 datum defects

2. With a known distance, an inner constraints datum for resolving the remaining 6 other datum defects

An inner constraints datum for resolving 7 datum defects is the best datum for the estimation of the conic constant because this parameter is scale-independent.

The first datum cannot be used for the estimation of radius of curvature because this parameter is scale-dependent. The scale is defined by a scale-bar with a known distance and its uncertainty.

2.3. Close-Range Photogrammetric Network Design by Heuristic Simulation

Previous research on this topic in close-range photogrammetry was done by Fraser 1984, 1992, 1996 who discussed the network design problem in close-range photogrammetry. Fritsch and Crosilla, 1990 performed first order design with an analytical method. Mason, 1994 used expert systems and Olague, 2002 used a genetic algorithm for the placement of matrix array cameras using heuristic computer simulations. Precision and reliability considerations in close-range photogrammetry, as a part of the network quality requirements, have been addressed by Gruen, 1978, 1980 and Torlegard, 1980. Considerations on camera placement for the determination of the additional parameters of the camera by using control points were addressed by Gruen and Beyer, 2001. The relation between highly redundant image acquisition and the respectively very high accuracy in point coordinates was already demonstrated by Amiri Parian, 2004 and Fraser et al., 2005.

The aim of heuristic simulation is to design an optimal close-range photogrammetric network with a precision which matches the required values from the previous step (SOD). In addition to the work space limits and the existing facilities for the placement and orientation of the camera the network should also be able to:

a) de-correlate (at least partially) the point coordinates with respect to the other parameters (the exterior orientation and additional parameters of the camera).

b) estimate additional parameters reliably

c) reduce the photogrammetric block triangulation error caused by the incidence angle of retro-reflective targets (reflectivity).

d) reduce the error of image target center (eccentricity) by selecting an appropriate location and orientation of the camera and a suitable target size. The image target center error is the error of the measured target center with respect to the physical target center because of the perspective projection effect.

Considering the existing facilities of Alcatel Alenia Space (with the capability to operate at very cold temperatures) a network was designed that satisfies the above 4 conditions.

Figure 2 shows the configuration of the camera stations with respect to the PR. The network consists of 70 stations with 1 image per station. The incidence angle of the camera optical axis with respect to the aperture of the PR is 30 degrees. With the assumption based on our previous measurement experience (Amiri Parian et al., 2006) that the internal accuracy of the camera system is 1/70 of a pixel the relative precision of the network is better than 1:1,000,000.

3. RESULTS OF REAL MEASUREMENTS

Previous measurements of the Planck reflectors were related to the Qualification Model of SR (SRQM) (Amiri Parian et al., 2006) which were performed in vacuum, at temperatures down to 95 Kelvin and at 13 epochs. In the measurement of SRQM, most of the targets fell off and were unstable during image acquisition because of loss of target adhesion in cold temperatures. From the experience of that measurement, suitable adhesion and type of targets were selected for the measurements of the flight models of the primary and secondary reflectors.

The Flight Model of Primary Reflector (PRFM) of the Planck telescope was measured by Alcatel Alenia Space France (AASF) under ESA-ESTEC contract according to the designed network. The PRFM was measured in vacuum and at temperatures down to 95 Kelvin, in total at 11 epochs. Approximately 2400 targets were stuck homogenously on the surface of the PR. The number of targets compared to the number of targets in the simulation (1000 targets) was increased. The monitoring of the small scale features of the PRFM and the availability of sufficient number of targets in cold temperatures in the case of target fall off were the reasons of using more targets than the estimated number in the design step.

The average number of missed targets because of falling off and instability was 9 targets per each epoch. From 2400 targets of the PRFM, approximately 100 targets were not used in the computation of the last (11) epoch.

Bundle block adjustment was done with the Limiting Error Propagation (LEP) method (Fraser, 1987) because of the large amount of object points (approximately 2400 targets). To investigate the relation of the Total Error Propagation (TEP) and the LEP in this network configuration, groups of re-sampled object points with 300, 450 and 600 targets were selected and bundle adjustment were run with the TEP and the LEP method. The precision from the LEP of these versions were better than the precisions from TEP by a factor of 1.2. This factor was used to convert the final LEP results to TEP results.

The configuration and the computation results of the network were the same for all epochs except at epoch 8, in which 2 images were acquired per station in order to enhance the precision. The overall precision of the real networks are in good agreement with the simulated network and is better than 1:1,000,000 for all epochs. At epoch 8 the overall precision was 1:1,350,000 which is better than the other networks by a factor of 1.35. The mean precision of the object point coordinates at

epoch 11 is 1.8 microns for XY-axis (lateral axes) and is 2.1 microns for Z-axis (depth axis). The overall redundancy of the network (0.97) is very high which enables the blunder detection reliably. The blunder detection was done automatically based on a dynamic threshold for the residuals which was computed from the RMS value of the image point residuals. The average condition number and the maximum isotropy of the network which show the isotropy of the precision were 0.66 and 0.51 respectively. Table 1 summarizes the results of the computations after conversion of LEP to TEP.
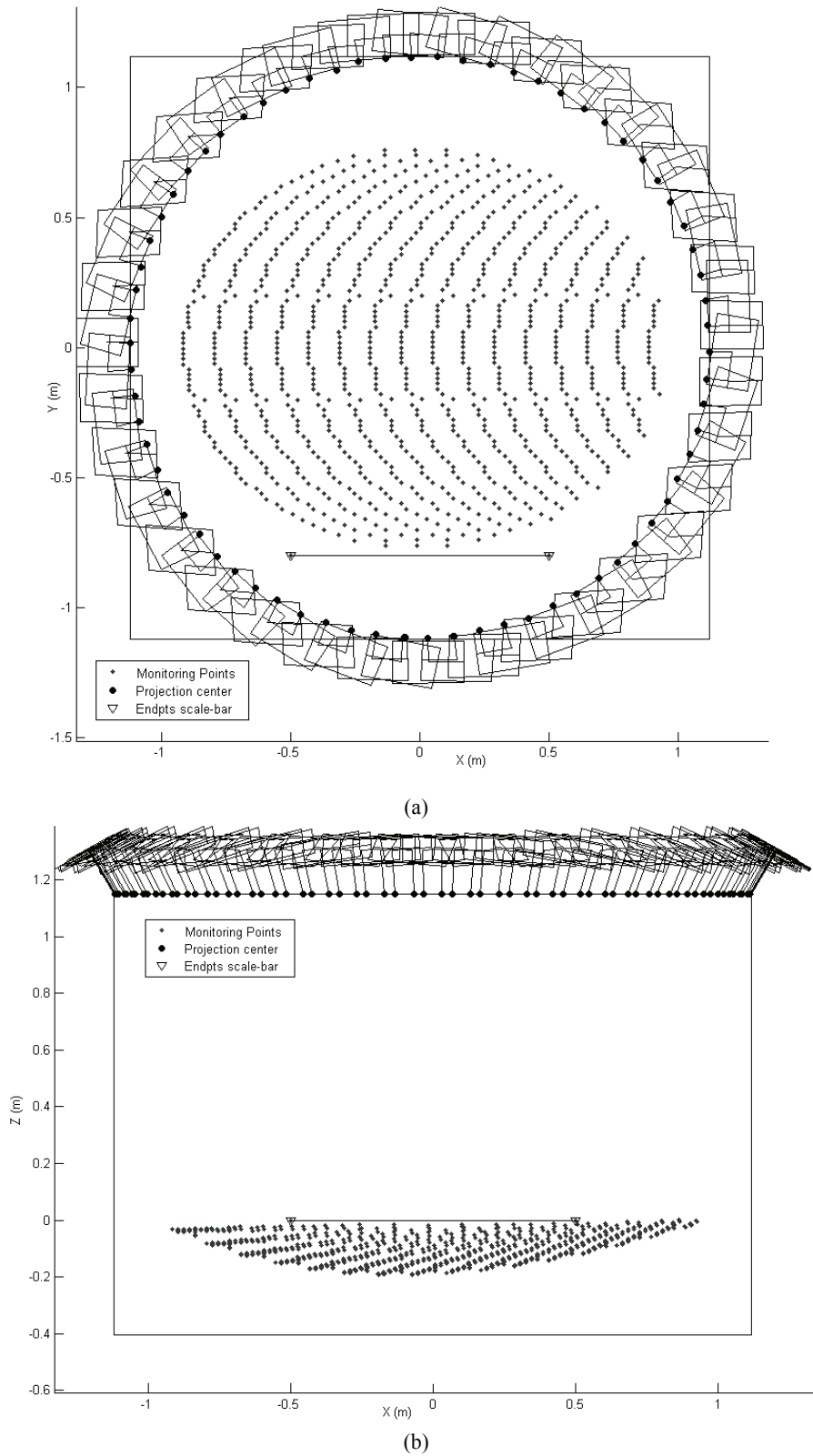

(a)

(b)

Figure 2. Network configuration for the PR. (a) XY-view and (b) XZ-view of the network.

Table 1. Results summary of the measurements at epoch M11 and M8.

	Epoch 11	Epoch 8
Number of images	*65*	*140*
Average number of points in each image	*2200*	*2213*
Average number of rays of each point	*62*	*130*
RMS value of the image point residuals	*0.011 (1/90) pixel*	*0.013 (1/76) pixel*
Maximum semi-axis of the error ellipsoid (one-sigma)	*3.2 microns*	*2.4 microns*
Mean precision along X, Y and Z axes (microns)	*1.7, 1.8, 2.1*	*1.2, 1.2, 1.7*
Overall precision of the target measurement (one-sigma)	*1:1,050,000*	*1:1,350,000*
Overall redundancy[1]	*0.97*	*0.98*
Average condition number[2] for each point	*0.66*	*0.66*
Maximum isotropy[3]	*0.51*	*0.47*

1 *Average redundancy number for each image point observation*

2 $Condition\ number = \dfrac{\lambda_{min}}{\lambda_{max}}\ with\ \lambda\ the\ semi-axis\ of\ the\ error\ ellipsoid$

3 $Isotropy = \dfrac{\max(\sigma_X, \sigma_Y, \sigma_Z) - \min(\sigma_X, \sigma_Y, \sigma_Z)}{mean(\sigma_X, \sigma_Y, \sigma_Z)}$

The extremely high accuracy could be achieved by highly redundant image acquisition. An average of 66 images were acquired in each epoch (except in epoch 8 in which 140 images were acquired) overlapping all each other and containing 2200 targets with an average number of 62 rays per point.

Through the analysis of the target center eccentricity in object and image space an optimal target size was selected. To decrease systematic errors caused by the eccentricity of the target center in object space, the rays with incidence angle greater than the criterion which was computed in the design step, were not used in the computations.

To compensate for systematic errors of the camera, Brown's additional parameters set (Brown 1976) with 8 Additional Parameters (APs) and 2 APs for correction of affinity and shear of the CCD-chip coordinate axes were applied. Figure 3 shows the image space pattern of the systematic errors which was modeled by APs. The amplitude of the residuals is in the order of 80 pixels.
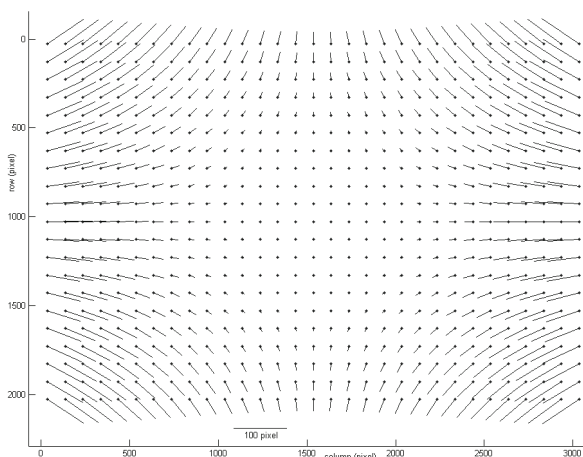

Figure 3. The image space pattern of the systematic errors of the camera.

The significance test of parameters was done with both one-dimensional and multi-dimensional tests. All APs are significant and no correlations higher than 0.90 present between

APs except for radial symmetrical lens distortions (3 parameters). No correlation higher than 0.85 is present between APs and object point coordinates and between APs and exterior orientation parameters of the camera. Therefore, the estimation of the object point coordinates is reliable taking into account the redundancy of the observations.

Environmental precautions were taken into account. By using thermo-sensors, a constant and homogeneous temperature was provided over different parts of the PRFM. In addition, since the tests were performed in vacuum, no vibration occurred because of air flow.

The optical parameters were estimated by the developed best-fit ellipsoid method and by choosing an appropriate datum. Since all targets are of the same type (with the same thickness) the best-fit ellipsoid was performed in the first step to estimate the parameters of the ellipsoid. These parameters were used for the determination of the normal vector to the surface of the PRFM. The thickness of the target and its standard deviation, which was estimated by measuring the profile of the targets with a stylus measuring equipment by ESA-ESTEC, were used to correct for the thickness of the target. The standard deviation of the target thickness and the point coordinates were used to estimate the point coordinates and their precision on the surface of the PRFM by error propagation. After compensation of the target thickness and computing the standard deviation of the point coordinates on the surface of the PRFM, the ellipsoid fitting was performed and optical parameters were estimated. Large residuals because of the target displacement were also eliminated from the computations.

4. CONCLUSIONS

Three steps of network design: SOD, FOD and ZOD were performed. In SOD the precision of the point coordinates was estimated from the requested precision of the optical parameters of the Primary Reflector of the Planck telescope. A least squares surface modeling for ellipsoid fitting was developed based on the given model of the reflector to relate the point coordinates to the optical parameters. FOD was performed by heuristic simulation to find an optimal configuration of camera stations in order to achieve the estimated precision of the point coordinates

in the previous design step (SOD). ZOD was performed in order to achieve the best possible precision of the optical parameters. An optimal close-range photogrammetric network was designed by heuristic simulation with a relative precision better than 1:1,000,000.

A real measurement of the PRFM was performed based on the designed network by Alcatel Alenia Space under ESA-ESTEC contract at 11 epochs with a coldest temperature at 95 Kelvin. The RMS error of the image point residuals was 1/90 pixel and the mean object point precision was 1.8 and 2.1 microns for the lateral and depth axes. This extremely high precision could be acquired by a strong geometrical network, the concept of hyper-redundancy, an efficient blunder detection method and advanced self-calibration.

REFERENCES

Amiri Parian, J., 2004. Close Range Photogrammetric Network Design Based on Micro-Cameras for Herschel Spacecraft. Technical report for the European Space Technology and Research Center (ESTEC), The Netherlands.

Amiri Parian, J., Gruen, A. and Cozzani, A., 2006. High Accuracy Deformation Monitoring of Space Structures by Heuristic Simulations. In: *Third IAG Symposium on Geodesy for Geotechnical and Structural Engineering and 12th FIG Symposium on Deformation Measurements*, Baden, Austria, p. 10.

Brown, D. C., 1976. The Bundle Adjustment – Progress and Prospects. In: *International Archive of Photogrammetry*, Helsinki, Finland, Vol. 21, Part B3, p. 33.

Fraser, C. S., 1984. Network Design Considerations for Non-Topographic Photogrammetry. *Photogrammetric Engineering and Remote Sensing*, 50(8), pp. 1115-1126.

Fraser, C. S., 1987. Limiting Error Propagation in Network Design. *Photogrammetric Engineering and Remote Sensing*, 53(5), pp. 487-493.

Fraser, C. S., 1992. Photogrammetric Measurement to One Part in a Million. *Photogrammetric Engineering and Remote Sensing*, 58(3), pp. 305-310.

Fraser, C. S., 1996. Network Design, Chapter 9. In: Atkinson, K. B. (editor), *Close Range Photogrammetry and Machine Vision*. Whittles Publishing, Roseleigh House, Latheronwheel, Caithness, Scotland, pp. 256-281.

Fraser, C. S., Woods, A. and Brizzi, D., 2005. Hyper Redundancy for Accuracy Enhancement in Automated Close Range Photogrammetry. *The Photogrammetric Record*, 20(111), pp. 205–217.

Fritsch, D. and Crosilla, F., 1990. First-Order Design Strategies for Industrial Photogrammetry. In: *SPIE*, Vol. 1395, Close-Range Photogrammetry Meets Machine Vision, pp. 432-438.

Grafarend, E., 1974. Optimization of Geodetic Networks. *Bollettino di Geodesia a Science Affini*, 33(4), pp. 351-406.

Gruen, A., 1978. Accuracy, Reliability and Statistics in Close-Range Photogrammetry. In: *Symposium of ISP*, Commission V, Stockholm, Sweden.

Gruen, A., 1980. Precision and Reliability Aspects in Close-Range Photogrammetry. In: *XIV Congress of ISP*, Commission V, Hamburg, Federal Republic of Germany, pp. 117-133.

Gruen, A. and Beyer, H., 2001. System Calibration Through Self-Calibration. In: Gruen, A. and Huang, T. S. (editors), *Calibration and Orientation of Cameras in Computer Vision*. Springer-Verlag, Berlin Heidelberg, pp. 172-180.

Mason, S., 1994. *Expert System-Based Design of Photogrammetric Networks*. Institute of Geodesy and Photogrammetry, ETH Zurich, Switzerland, No. 53, PhD Thesis.

Olague, G., 2002. Automated Photogrammetric Network Design Using Genetic Algorithms. *Photogrammetric Engineering and Remote Sensing*, 68(5), pp. 423-431.

Torlegard, K., 1980. On Accuracy Improvement in Close-Range Photogrammetry. In: *Proceedings of Industrial and Engineering Survey Conference*, London, England.

Wimmer, H., 1982. Second Order Design of geodetic networks by an iterative approximation of a given criterion matrix. In: *Deutsche Geodaetische Kommission*, Reihe B, Heft 258/III, pp. 112-127.